Photonic Crystals Fabricated Using Patterned Nanorod Arrays**

By *Xudong Wang*, *Curtis Neff*, *Elton Graugnard*, *Yong Ding*, *Jeffrey S. King*, *Lawrence A. Pranger*, *Rina Tannenbaum*, *Zhong L. Wang*,* and *Christopher J. Summers**

Two-dimensional (2D) photonic crystal (PC) slabs have attracted much research interest due to the relative ease of achieving a full photonic bandgap.[1,2] A wide variety of applications in optoelectronics have been explored using 2D PCs, such as waveguides,[3] superprisms,[4] laser diodes,[5] and photonic integrated circuits.[6] Traditionally, 2D PCs are fabricated by electron-beam lithography, which is a top–down process that is expensive and limited to relatively small areas;[7] these factors possibly hinder the application and commercialization of 2D PCs. A combination of top–down and bottom–up processes has been attempted, in which a 2D pattern is created by lithography followed by a self-assembly process to achieve the final structure.[8] Recently, by using monolayer self-assembly (MSA) of polystyrene (PS) submicrometer spheres to define a pattern, a catalyst-controlled selective growth technique has been applied to make 2D periodic arrays, such as hexagonal-patterned carbon nanotubes[9] and ZnO nanorods.[10] This is a simple and cost-effective approach for growing quasi-one-dimensional (quasi-1D) nanostructure arrays on a relatively large scale. However, these as-synthesized 1D nanostructures have a large percentage of air space and a vanishing photonic bandgap, and are not suitable for photonic applications. We present here a bottom–up process for fabricating 2D PC slabs starting with patterned ZnO nanorod arrays that were conformally coated with TiO_2 by template-assisted atomic layer deposition (ALD), a powerful technique for fabricating a variety of nanostructures, such as inverse opals,[11,12] one-dimensional nanostructures,[13] and nanobowl arrays.[14] The space between the ZnO nanorods was partially filled with TiO_2, thus forming a continuous ZnO/TiO_2 matrix with a highly ordered air-hole array. This periodic structure showed a reflection peak at the theoretically predicted bandgap region, while the near-UV emission of ZnO was unaffected by the TiO_2 coating. This technique demonstrates an effective and economical bottom–up process for 2D PC fabrication.

Our objective was to make a photonic crystal with high refractive-index contrast, which was achieved by a two-step process: growth of patterned nanorod arrays with large air holes, then infiltration of the nanorod arrays with TiO_2 to form an air/TiO_2/nanorod photonic crystal. In the first step, a continuous hexagonal gold nanoparticle pattern was formed on a sapphire substrate. The aligned ZnO nanorods were then grown using the gold pattern as a catalyst in a tube furnace at elevated temperature.[10] A honeycomb-like pattern of dense and well-aligned ZnO nanorod arrays was produced, as shown by the scanning electron microscopy (SEM) image in Figure 1a. The diameter and length of the ZnO nanorods were controlled by the thickness of the gold catalyst layer and the growth time. For a growth time of 15 min, the length of the ZnO nanorods was ~500 nm and their diameters ranged from ~20–30 nm.

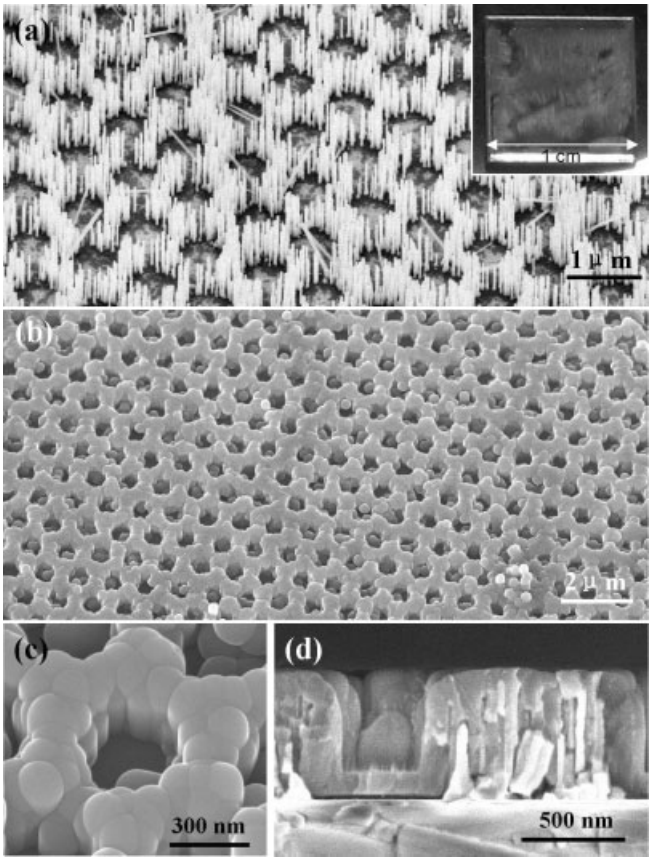

Figure 1. SEM images of the TiO_2/ZnO quasi-2D photonic crystal structure. a) Short and densely aligned ZnO nanorod array on a sapphire substrate. Inset: An optical image of the aligned ZnO nanorods over a large area. b) Low-magnification SEM image of the TiO_2-coated ZnO nanorod array. c) High-magnification SEM image showing a single air hole surrounded by ZnO nanorods imbedded in TiO_2 walls. d) Cross section of the TiO_2-coated ZnO nanorod array.

[*] Prof. Z. L. Wang, Prof. C. J. Summers, X. D. Wang, C. Neff, Dr. E. Graugnard, Dr. Y. Ding, Dr. J. S. King, L. A. Pranger, Prof. R. Tannenbaum
School of Materials Science and Engineering
Georgia Institute of Technology
Atlanta, GA 30332-0245 (USA)
E-mail: zhong.wang@mse.gatech.edu; chris.summers@mse.gatech.edu

[**] We are grateful for financial support from a US NSF grant DMR-9733160, the MURI program from an ARO grant DAAD19-01-1-0603, and the NASA URETI program.

 DOI: 10.1002/adma.200500546

ADVANCED MATERIALS

In the second step, the ZnO nanorods were uniformly coated by a layer of TiO_2 using low-temperature ALD. The SEM image of the TiO_2-coated ZnO nanorod array is shown in Figure 1b. All of the ZnO nanorods are coated with TiO_2, forming a continuous dielectric film patterned with a hexagonal air-hole array. This configuration is very close to the structure of a 2D PC slab that can exhibit a full photonic bandgap. Because the height of this slab is ~600 nm, which is less than the minimum height for guiding infrared radiation, the structure is a quasi-2D PC structure.

The TiO_2-coated surface is presented by the high-magnification SEM image shown in Figure 1c. The interior surface of the air holes is actually a combination of closely spaced dielectric cylinders, as a result of the uniform growth of TiO_2 around each ZnO nanorod. Figure 1d is a cross-section of the TiO_2/ZnO 2D PC, which clearly shows that the space between the ZnO nanorods is completely filled by TiO_2 because of the deep penetration of the ALD reactants. Owing to the uniform length of the ZnO nanorods, the TiO_2 coating exhibits a flat top surface. The thickness of the conformal TiO_2 coating measured at the substrate region is ~110 nm, which is uniform over all features, i.e., over both the sapphire substrate and the vertical ZnO nanorods. Since the ZnO nanorods are a few micrometers in length, the ~110 nm thick layer of TiO_2 deposited on the substrate does not affect the entire structure of the 2D PC. The total thickness of the quasi-2D PC is ~600 nm, including the thickness of the TiO_2 layer on the substrate. The space between the TiO_2 layer and the substrate (see Fig. 1d) was created when the sample was cleaved for the SEM study.

Transmission electron microscopy (TEM) was used to characterize the crystal structure of the TiO_2-coated ZnO nanorods. The TEM sample was acquired at a broken edge as shown in Figure 1d. Most of the TiO_2 layer is fractured off, and the ZnO nanorod observed in the TEM image of Figure 2a is covered only by a very thin layer of TiO_2. The dark tip at the front of the ZnO nanorod is the gold catalyst, which has a similar size to the nanorod. The corresponding diffraction pattern reveals that the growth of the ZnO nanorod is along the [0001] direction. Other than the diffraction spots from the ZnO, no spots are observed, which confirms that the TiO_2 coating is amorphous. Further evidence of the film structure is shown by the high-resolution TEM picture in Figure 2b. The lattice fringes correspond to the (0002) planes of the ZnO crystal, on top of which a clear TiO_2 amorphous layer is shown. At the interfacial region, no lattice deformation is observed. Although ZnO and TiO_2 can easily form an alloy at elevated temperatures,[15] the films are stable at the low TiO_2 deposition temperature of 100 °C. The presence of the elements was confirmed by energy-dispersive X-ray spectroscopy (EDS) carried out on the edge region. As shown in Figure 2c, strong signals from Zn, Ti, and O are recorded together with a small amount of Cl, which is due to the incomplete ALD reaction between $TiCl_4$ and H_2O at the relatively low deposition temperature.

The photonic band structure of the fabricated photonic crystal was studied theoretically and experimentally. Based on

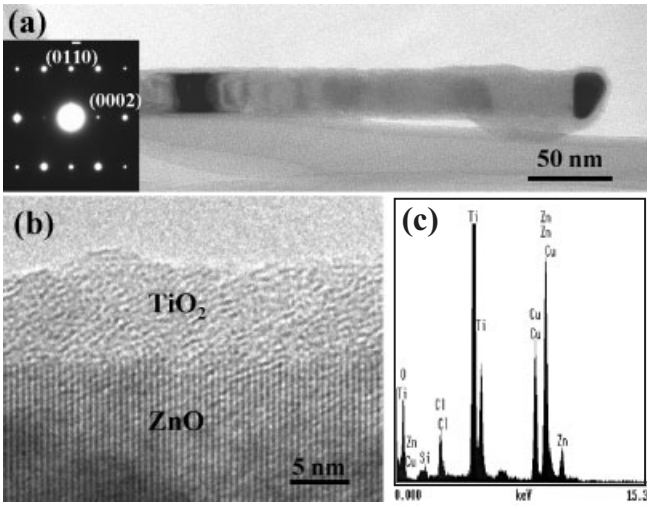

Figure 2. a) Low-magnification TEM image showing a ZnO nanorod removed from the TiO_2 coating and the corresponding electron diffraction pattern (inset). b) High-magnification TEM image of the side region of the ZnO nanorod showing an amorphous TiO_2 film covering the ZnO crystal. c) EDS spectrum of the TiO_2-coated region.

the experimental configuration of the TiO_2-coated ZnO nanorod arrays, the band structure was first calculated for the model presented in Figure 3a, in which a 2D PC structure with a triangular lattice of truncated air holes was assumed. The dielectric matrix of the PC was treated as a uniform media with an average refractive index of amorphous TiO_2 and ZnO weighted by their volume ratios. In our case, by measuring ten randomly recorded SEM images, the density of ZnO nanorods was counted as ~120 μm^{-2}, and their average diameter and length were 30 nm and 500 nm, respectively. The volume of the TiO_2 matrix was estimated by assuming the air holes were cylindrical, with an average distance between two neighboring air holes of $a = 900$ nm and an average air-hole internal diameter of ~480 nm. Thus, the volume fraction of ZnO was calculated to be 8 %. Considering the refractive indexes of ZnO and TiO_2 to be 1.99 and 2.25 in the infrared region, respectively, the effective refractive index was given by $n = 1.99 \times 8\,\% + 2.25 \times (1 - 8) = 2.23$. Similarly, the average dielectric constant of the matrix was estimated to be $\varepsilon = 4.97$. The following structural data were used in the calculation of the 2D PC band structure: lattice parameter $a = 900$ nm; air-hole internal diameter $d = 480$ nm; slab thickness $h = 600$ nm. Then the radius and slab thickness, in terms of the lattice parameter, were given by: $r = 0.267\,a$ and $h = 0.67\,a$, respectively.

Calculations were performed by means of the plane wave expansion method using a publicly available code[16] with a supercell as depicted in Figure 3a. Centered in the vertical dimension of the supercell is the 2D PC slab mounted on a sapphire substrate ($\varepsilon = 2.96$) and surrounded above by air, all of which are infinitely extended in the y and z directions. Because of the nature of the calculation, the supercell is repeated in the x direction; hence, the air space between the slabs must be sufficient so that coupling of the guided modes

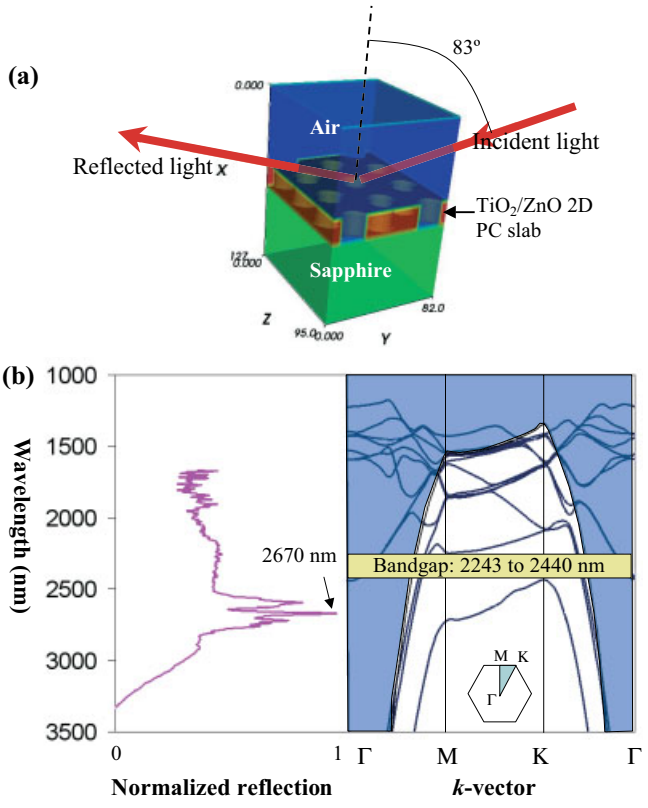

Figure 3. a) A schematic model of the TiO2/ZnO quasi-2D PC used for calculations; the reflection measurement condition is also illustrated. b) Left: reflection spectrum of the TiO_2/ZnO quasi-2D PC slab after the reference was removed. Right: calculated photonic band structure of the quasi-2D PC slab.

between the slabs is minimized. This means that the modes that are not guided in the slab couple to one another, and their solutions become part of the background continuum of modes that is shown by the shaded region of the band structure in Figure 3b. The band structure for the transverse electric (TE)-like solutions is shown, and a pseudo-bandgap region between the first and second bands is predicted in the normalized frequency range, $\omega a/(2\pi c)$, from 0.367 to 0.401, which corresponds to wavelengths from 2440 to 2243 nm. In this frequency range, there will be a dip in the photon density of states that will manifest itself as a peak in the reflectivity spectrum.

It was reported that the photonic band structure can be determined by reflection spectra,[17] in which the reflection peaks at different incident angles compose a large part of the band configuration. In our experiments, the photonic bandgap of the quasi-2D PC slab was measured by infrared spectroscopy at a large, fixed incident angle (83°) to the normal direction, so as to enhance the interaction between the light and the lattice. Reflection spectra were acquired from both the TiO_2/ZnO quasi-2D PC slab and a thin layer of amorphous TiO_2 deposited on a flat sapphire substrate, which was used as a reference. The left-hand side of Figure 3b is the normalized reflection spectrum after subtracting the reference spectrum. A reflection peak was observed at 2670 nm with a full width at half maximum of ~220 nm. Comparing this peak valve with the calculated bandgap center at 2342 nm gives a mismatch of ~12 %, which may be accounted for by the following factors: The theoretical calculation was based on several assumptions and simplifications, which can change the distribution of the band structure. The theoretical bandgap was calculated for light transmitted within the 2D PC slab perpendicular to the normal direction, while experimentally the light was reflected off the slab surface at a large angle. This non-perpendicular light transportation causes a shift in the wavelength of the reflected light, which corresponds to the band distribution at a certain transportation angle.[17,18] According to this, the data from this one fixed angle measurement is not sufficient to generate the whole band structure to match our theoretical calculation; however, the reflection peaks from the spectrum are able to clearly show the existence of the photonic bandgap. Experimentally, there are a few issues associated with the relatively noisy spectra that could contribute to the mismatch. Due to the large lattice parameter, the bandgap lies at fairly long wavelengths, where chemical species such as H_2O can also influence the reflection signal. The short length of this quasi-2D PC limits the light–lattice interaction, and as shown in Figures 1a,c, the air holes are not perfectly cylindrical, which results in random scattering effects.

As predicted by the theoretical calculation, the bandgap can be moved into the visible region by changing the lattice parameter to ~100 nm. Being supported by single-crystal ZnO nanorods, the matrix can be rigid even when its thickness becomes as thin as 30 nm, which is required for fabricating a 2D PC with a bandgap in the visible spectral region by this technique. Achieving such a small feature is very expensive using lithography-based techniques. Therefore, through a bottom–up process, this technique created a new pathway for the much more economical, large-scale fabrication of 2D PC devices capable of operating over a wide wavelength range.

In order to investigate the light-emitting properties of the quasi-2D PC slab with embedded ZnO nanorods, the photoluminescence (PL) of the ZnO nanorod array was measured before and after TiO_2 coating. As shown in Figure 4, the bare ZnO nanorod array has a PL peak at 384 nm. After being coated with a ~110 nm TiO_2 layer, a PL peak with almost the same intensity was still observed at 383 nm. A transmittance spectrum was also measured on a 100 nm thick, amorphous TiO_2 thin layer from the near-UV to the visible region. As shown in Figure 4c, amorphous TiO_2 exhibits an enhanced transmission at 380–390 nm, which matches the PL peak from ZnO nanorods very well. Thus, the near-UV emission from the ZnO nanorods can be transmitted through the TiO_2 coating with little loss and is expected to show an identical PL peak, with comparable intensity, at the same wavelength as the non-coated ZnO nanorods. In addition, ZnO nanorods can be excited by UV radiation to lase at a wavelength of ~385 nm,[19] thus, the TiO_2 coating will not affect the optical performance of the ZnO nanorods.

ADVANCED MATERIALS

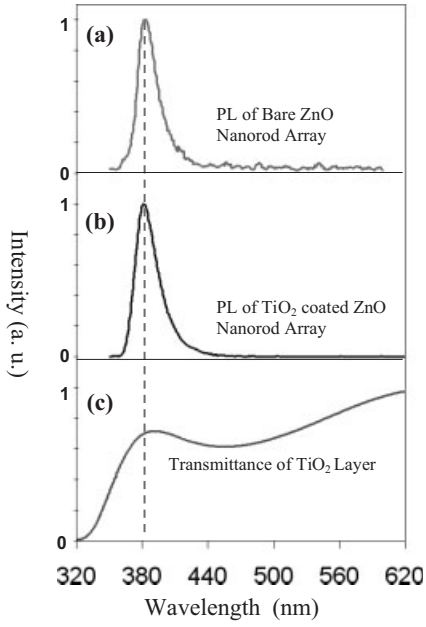

Figure 4. Photoluminescence spectra of a) a bare ZnO nanorod array and b) a TiO_2/ZnO quasi-2D PC slab. c) Transmission spectrum of an amorphous TiO_2 layer.

In summary, we present an completely bottom–up process for the fabrication of luminescent TiO_2/ZnO 2D PCs using a patterned and aligned ZnO nanorod array as a coating template. This periodic structure showed a reflection peak close to the theoretically predicted bandgap region. The photoluminescence of ZnO was not quenched by the TiO_2 coating. The bandgap can be controlled by varying the period of the PS sphere template, which is feasible down to ~100 nm; thus, a 2D PC with a bandgap in the visible light region is possible. The technique is a self-assembly process that is entirely bottom–up and can be effectively and economically scaled up for large-sized 2D PC fabrication.

Experimental

PS spheres (10 % in water) with a diameter of 890 nm were self-assembled to make a monolayer mask on a $(11\bar{2}0)$ sapphire substrate surface [10]. The surface was then covered with a layer of gold ~3 nm thick. By removing the PS spheres with toluene, a continuous hexagonal gold nanoparticle pattern was formed on the substrate. ZnO nanorods were grown using the gold pattern as a catalyst through a vapor–liquid–solid process. The source materials, a mixture of equal amounts (by weight) of ZnO and graphite powders, were loaded in an alumina boat, which was located at the center of an alumina horizontal tube furnace. Argon was used as the carrying gas at a flow rate of 25 sccm. The substrates were placed ~10 cm downstream from the source materials. The horizontal tube furnace was heated to 950 °C at a rate of 50 °C min^{-1}, and the temperature was held for 30 min under a pressure of 300 mbar (1 mbar ≈ 0.1 kPa). Then the furnace heating was stopped and the system was slowly cooled to room temperature under an argon flow. Atomic layer deposition was also carried out in a tube furnace using a quartz tube as the reaction chamber. $TiCl_4$ and H_2O were used as precursors. As-synthesized aligned ZnO nanorod arrays were placed at the center of the ALD chamber, which was kept at 100 °C during the entire growth process. Pulses of $TiCl_4$ vapor and H_2O vapor were introduced sequentially into the chamber under a vacuum of ~2 torr (1 torr ≈ 133 Pa). The pulse duration was 4 s, and the pulses were separated by a N_2 gas purge for 10 s. The growth per cycle was ~0.1 nm, which was determined experimentally from the planar growth per cycle of TiO_2 on natively oxidized Si(100) substrates at 100 °C [20].

The products were characterized by using a LEO 1530 field-emission gun (FEG) scanning electron microscope operated at 5 kV and a Hitachi HF200 transmission electron microscope operated at 200 kV. EDS analysis was performed during the TEM measurements. The reflection spectrum was measured by a Nexus 870 Fourier-transform infrared instrument. The incident angle of the infrared beam was fixed at 83° to the normal direction, and the reflected signals were collected by an infrared detector positioned at the same angle. Photoluminescence (PL) measurements were performed at room temperature using a 337 nm N_2 pulse laser as an excitation light source. The laser was run at 15 Hz, 800 ps pulse duration with an average energy of 50 mW.

Received: March 15, 2005
Final version: April 20, 2005
Published online: July 26, 2005

[1] T. F. Krauss, R. M. De La Rue, S. Brand, *Nature* **1996**, *383*, 699.
[2] A. Rosenberg, R. J. Tonucci, H. B. Lin, A. J. Campillo, *Opt. Lett.* **1996**, *21*, 830.
[3] W. Park, C. J. Summers, *Appl. Phys. Lett.* **2004**, *84*, 2013.
[4] H. Kosaka, T. Kawashima, A. Tomita, M. Notomi, T. Tamamura, T. Sato, S. Kawakami, *Phys. Rev. B* **1998**, *58*, R10 096.
[5] H. Hirayama, T. Hamano, Y. Aoyagi, *Appl. Phys. Lett.* **1996**, *69*, 791.
[6] J. D. Joannopoulos, P. R. Villeneuve, S. Fan, *Nature* **1997**, *386*, 143.
[7] E. Chow, S. Y. Lin, S. G. Johnson, P. R. Villeneuve, J. D. Joannopoulos, J. R. Wendt, G. A. Vawter, W. Zubrzycki, H. Hou, A. Alleman, *Nature* **2000**, *407*, 983.
[8] T. Mårtensson, P. Carlberg, M. Borgström, L. Montelius, W. Seifert, L. Samuelson *Nano Lett.* **2004**, *4*, 699.
[9] K. Kempa, B. Kimball, J. Rybczynski, Z. P. Huang, P. F. Wu, D. Steeves, M. Sennett, M. Giersig, D. V. G. L. N. Rao, D. L. Carnahan, D. Z. Wang, J. Y. Lao, W. Z. Li, Z. F. Ren, *Nano Lett.* **2003**, *3*, 13.
[10] X. D. Wang, C. J. Summers, Z. L. Wang, *Nano Lett.* **2004**, *4*, 423.
[11] J. S. King, C. W. Neff, C. J. Summers, W. Park, S. Blomquist, E. Forsythe, D. Morton, *Appl. Phys. Lett.* **2003**, *83*, 2566.
[12] J. S. King, E. Graugnard, C. J. Summers, *Adv. Mater.* **2005**, *17*, 1010.
[13] H. Shin, D. K. Jeong, J. Lee, M. M. Sung, J. Kim, *Adv. Mater.* **2004**, *16*, 1197.
[14] X. D. Wang, E. Graugnard, J. S. King, Z. L. Wang, C. J. Summers, *Nano Lett.* **2004**, *4*, 2223.
[15] G. Marcì, V. Augugliaro, M. J. López-Muñoz, C. Martín, L. Palmisano, V. Rives, M. Schiavello, R. J. D. Tilley, A. M. Venezia, *J. Phys. Chem. B* **2001**, *105*, 1026.
[16] S. G. Johnson, J. D. Joannopoulos, *Opt. Express* **2001**, *8*, 173.
[17] V. N. Astratov, D. M. Whittaker, I. S. Culshaw, R. M. Stevenson, M. S. Skolnick, T. F. Krauss, P. M. De La Rue, *Phys. Rev. B* **1999**, *60*, R16 255.
[18] D. Coquillat, J. Torres, D. Peyrade, R. Legros, J. P. Lascaray, M. Le Vassor d'Yerville, E. Centeno, D. Cassagne, J. P. Albert, Y. Chen, R. M. De La Rue, *Opt. Express* **2004**, *12*, 1097.
[19] M. H. Huang, S. Mao, H. Feick, H. Yan, Y. Wu, H. Kind, E. Weber, R. Russo, P. Yang, *Science* **2001**, *292*, 1897.
[20] J. S. King, D. Heineman, E. Graugnard, C. J. Summers, *Appl. Surf. Sci.* **2005**, *244*, 511.

